Acupuncture and Herbal Medicine

Tetramethylpyrazine attenuates chronic intermittent hypoxia-exacerbated diabetic atherosclerosis: a mechanistic study of the IRE1α-XBP1 signaling pathway

Binyu Luo[1,2], Wenting Wang[1], Yiwen Li[3], Jing Cui[1], Qian Xu[1], Mengmeng Zhu[1], Yanfei Liu[1,4], Yue Liu[1,*]

[1]National Clinical Research Center for Chinese Medicine Cardiology, Xiyuan Hospital, Chinese Academy of Chinese Medical Sciences, Beijing, China; [2]Quzhou College of Technology, Quzhou, Zhejiang, China; [3]Medical Experimental Center, China Academy of Chinese Medical Sciences, Beijing, China; [4]The Second Department of Gerontology, Xiyuan Hospital, China Academy of Chinese Medical Sciences, Beijing, China

Abstract

Objective: A complex relationship exists between obstructive sleep apnea syndrome and diabetes mellitus (DM). Chronic intermittent hypoxia (CIH), which is a core pathological feature of obstructive sleep apnea syndrome, may play an important role in the onset and development of DM-related atherosclerosis (DM-AS). This study aimed to investigate the mechanism of action of tetramethylpyrazine (TMP) in CIH-associated DM-AS.

Methods: *In vivo*, a DM-AS mouse model was established by intraperitoneal injection of streptozotocin combined with a high-fat diet. They were exposed to CIH or normoxic conditions for 8 weeks and received different doses of TMP, rosuvastatin, toyocamycin, and purified water. Glycolipid metabolism, inflammation levels, degree of aortic AS, and expression levels of endoplasmic reticulum stress (ERS) and autophagy proteins were examined in mice. *In vitro*, human umbilical vein endothelial cells (HUVECs) were treated with high glucose and fat in combination with insulin to establish an insulin-resistant cell model (HUVEC-IR). After pretreatment with 4μ8C (IRE1 inhibitor) and different doses of TMP, intermittent hypoxic intervention was performed. Changes in cell morphology, proliferative activity, glucose consumption, and ability to migrate were observed, and the expression levels of ERS and autophagy proteins were detected.

Results: *In vivo* experiments showed that CIH significantly increased blood glucose levels and Homeostasis Model Assessment of Insulin Resistance (HOMA-IR) ($P < 0.001$ or $P < 0.05$), low-density lipoprotein cholesterol (LDL-C) content ($P < 0.001$), and the levels of three inflammatory factors [interleukin-1 beta (IL-1β), IL-6, and tumor necrosis factor-alpha (TNF-α)] in the mice ($P < 0.001$) compared with those of the mice with DM alone; moreover, the aortic atherosclerotic (AS) plaque area in CIH mice was significantly enlarged ($P < 0.001$). Western blotting results showed that the expressions of aortic IRE1α, XBP1s, Beclin1, and LC3A proteins were significantly increased in CIH mice compared with DM mice ($P < 0.05$). After treatment with different doses of TMP, rosuvastatin calcium, and toyocamycin, serum inflammation and lipid levels and plaque area were significantly reduced in mice ($P < 0.001$ and $P < 0.001$, respectively). The expression levels of aortic XBP1s, Beclin1, and LC3A were reduced in TMP- and toyocamycin-treated mice ($P < 0.05$). In the *in vitro* experiments, compared with normoxic cells, the cells treated with intermittent hypoxia (IH) showed a significant decrease in cell migration distance ($P < 0.05$), a significant increase in apoptosis rate ($P < 0.001$), a substantial increase in proliferation inhibition rate ($P < 0.001$), a significant increase in the levels of XBP1s and LC3A proteins ($P < 0.05$), and an increase in the number of autophagic vesicles/lysosomes, as observed under transmission electron microscopy. After treatment with different doses of TMP and 4μ8C, cell morphology was significantly restored, apoptosis rate significantly reduced ($P < 0.001$), and XBP1s, Beclin1, and LC3A expressions significantly inhibited ($P < 0.05$).

Conclusion: CIH promoted the onset of DM-AS, whereas TMP attenuated ERS and excessive autophagy by modulating the IRE1α-XBP1 signaling pathway and inhibiting XBP1 splicing, thereby ameliorating DM-AS exacerbated by CIH.

Keywords: Arteriosclerosis, Diabetes, Intermittent hypoxia, IRE1α-XBP1, TMP

Graphical abstract: https://links.lww.com/AHM/A170.

Binyu Luo and Wenting Wang are co-first authors.

**Corresponding author. Yue Liu, E-mail: liuyueheart@hotmail.com.*

Received 21 December 2024 / Accepted 25 March 2025

How to cite this article: *Luo BY, Wang WT, Li YW, Cui J, Xu Q, Zhu MM, Liu YF, Liu Y. Tetramethylpyrazine attenuates chronic intermittent hypoxia-exacerbated diabetic atherosclerosis: a mechanistic study of the IRE1α-XBP1 signaling pathway. Acupunct Herb Med 2025;5(2): 160–172. DOI: 10.1097/HM9.0000000000000154*

Copyright © 2025 Tianjin University of Traditional Chinese Medicine. This is an open-access article distributed under the terms of the Creative Commons Attribution-Non Commercial-No Derivatives License 4.0 (CCBY-NC-ND), where it is permissible to download and share the work provided it is properly cited. The work cannot be changed in any way or used commercially without permission from the journal.

Introduction

Obstructive sleep apnea syndrome (OSAS) is an independent risk factor for atherosclerosis (AS) because it promotes the onset of various cardiovascular diseases and increases the risk of death[1–3]. Patients with OSAS often have diabetes mellitus (DM), with worse glycemic control observed in more severe cases[4–5]. DM and OSAS, considered as "risk equivalents" for coronary heart disease, share a complex relationship that affects AS onset and progression. However, the specific underlying mechanisms have not been elucidated.

Intermittent hypoxia (IH), a hallmark of OSAS, is independently associated with metabolic dyslipidemia and exacerbates AS in the presence of abnormal glucose metabolism[6–7]. Recent studies have highlighted the roles of endoplasmic reticulum stress (ERS) and autophagy in chronic intermittent hypoxia (CIH)-mediated diabetic vascular endothelial injury and AS development[8]. The unfolded protein response (UPR) in ERS is triggered by the activation of transcription factor 6 (ATF6), inositol-requiring enzyme 1 (IRE1), and protein kinase R-like endoplasmic reticulum kinase (PERK). There are two isoforms of IRE1, namely IRE1α and IRE1β. IRE1α is expressed in the endothelial cells, vascular smooth muscle cells, and macrophages in AS plaques; it is an important sensor in UPR[9]. IRE1 undergoes autophosphorylation following dissociation from glucose-regulated protein 78. Phosphorylated IRE1α acts as a nucleic acid endonuclease and promotes the translation of active X-box binding protein 1 (XBP1), that is, spliced XBP1 (XBP1s) proteins[10]. XBP1 upregulates the expression of ERS-related proteins and promotes the degradation of misfolded proteins. IRE1α-mediated XBP1 mRNA activates microtubule-associated proteins 1A/1B light chain 3B (LC3B) to promote endothelial autophagy by regulating the transcription of the Beclin1 gene, an autophagy regulator; meanwhile, the silencing of XBP1 expression in endothelial cells eliminates endostatin-induced autophagy[11]. In addition, XBP1s affect macrophage autophagy and cell survival by regulating the transcription of Beclin1[12]. The interaction between the IRE1α-XBP1 signaling pathway and autophagy may be a potential novel therapeutic target for CIH-mediated DM-AS.

Recently, extensive research has been conducted on the anti-AS effects of traditional Chinese medicine (TCM). In clinical practice, it has been observed that patients with both OSAS and DM are primarily obese males, often experiencing symptoms like chest tightness, gastric distress, blue lips, purple tongue with ecchymosis, astringent pulse, and other indicative signs of blood stasis. Moreover, there exists a correlation between symptom severity and the incidence of vascular complications[13]. In addition, patients with OSAS and DM often exhibit hypercoagulability, which can lead to thrombosis[14] and development of AS. This pathological process resembles the concept of "blood stasis" in TCM. Tetramethylpyrazine (TMP), extracted from *Ligusticum sinense* cv. Chuanxiong, a common Chinese herbal medicine known for promoting blood circulation and eliminating blood stasis, demonstrates various anti-AS effects such as lipid metabolism regulation, anti-inflammatory properties, and antioxidant effects[15]. Clinical studies have indicated that TMP is effective for treating various DM-related vascular complications, including coronary heart disease, carotid AS, and prothrombotic state[15–16]. Besides, TMP alleviated insulin resistance (IR) and oxidative stress in an induced IR model of 3T3-L1 cells by modulating the sterol regulatory element-binding protein 1c/fatty acid synthase (SREBP-1c/FAS) pathway[17], as well as inhibiting excessive ERS stimulation and abnormal expression levels of IRE1α and XBP1[18]. However, the specific role of TMP in CIH-mediated DM-AS and its regulatory effects on the IRE1α-XBP1 pathway and autophagy remain unclear.

This study investigated the interaction between ERS and autophagy, focusing on the relationship between the IRE1α-XBP1 signaling pathway and autophagy. An ApoE$^{-/-}$ mouse model combining CIH and DM-AS was established *in vivo*, and an IR model was induced in human umbilical vein endothelial cells (HUVECs) *in vitro* through a combination of IH and high glucose and high fat (HGHF). The study aimed to elucidate the effects of the IRE1α-XBP1 signaling pathway and autophagy interaction on the development of AS induced by CIH and DM, as well as the potential intervention and molecular mechanisms of TMP. Furthermore, the study sought to provide evidence for TCM use for promoting blood circulation and stasis removal in the treatment of vascular lesions of AS secondary to OSAS and DM. The previous establishment of mature cells and animal models of IH intervention[7] provided a basis for this study.

Materials and methods

Animals

ApoE$^{-/-}$ (strain C57BL/6J) and C57BL/6J normal mice were purchased from Jiangsu GemPharmatech Co., Ltd., Nanjing, China (License No.: SCXK(SU)2018-0008). In total, 105 7-week-old male ApoE$^{-/-}$ mice weighing 18 to 20 g and 15 C57BL/6J mice of the same genetic background and weight range were selected. All mice were housed in a specific pathogen-free (SPF) animal facility (with sterilized water and chow) at a temperature of (22 ± 2)°C, humidity of (55 ± 5)%, and a 12-h day/night (light/dark) cycle. Acclimatization was performed for 1 week before the start of the formal experiments. ApoE$^{-/-}$ mice were fed with high-fat feed (7% cholesterol, 0.5% sodium taurocholate, 10% lard, 5% egg yolk powder, and 77.5% basal chow), and C57BL/6J mice were fed with regular feed. This animal study was approved by the Animal Ethics Committee of Xiyuan Hospital, China Academy of Chinese Medical Sciences (2021XLC046-1).

Animal experiment protocol

ApoE$^{-/-}$ mice were fed with high-fat chow for six consecutive weeks; afterward, they were randomly divided into normoxic control group 1 (N1), normoxic control group 2 (N2), CIH model group (CIH), low-dose TMP group (TMPL), high-dose TMP group (TMPH), toyocamycin group (XBP1 inhibitor, ACT), and rosuvastatin calcium group (ROS) (n = 12). Twelve C57BL/6J mice were fed with normal standard chow and served as the blank

control group (CON). Except for mice in the CON and N1 groups, which were injected intraperitoneally with an equal volume of pure water, mice in the remaining groups were injected intraperitoneally with a small dose of streptozotocin (STZ, 30 mg/kg, Sigma, Texas, USA.) for five consecutive days to induce DM fasting blood glucose (FBG) ≥11.1 mmol/L was regarded as successful modeling[19–20]. Mice from the CIH, TMPL, TMPH, ACT, and ROS groups were subjected to CIH intervention in a hypoxic incubator for 8 weeks. Specifically, >99% nitrogen (N_2) was introduced into the YCP-160D hypoxic animal incubator until the oxygen concentration reached (10 ± 0.5)%, which was maintained for approximately 90 seconds per cycle; afterward, >99% O_2 was injected into the incubator until the oxygen concentration was increased to (21 ± 0.5)% and maintained for approximately 90 seconds. One hypoxia-reoxygenation cycle lasted for 180 seconds (8 AM to 4 PM, 8 h/day)[7]. The mice received oral administration of equal volumes of pure water, low-dose TMP (600 mg/kg; Hebei Dongfeng Pharmaceutical Co., Ltd., Handan, China), high-dose TMP (1,200 mg/kg; Hebei Dongfeng Pharmaceutical Co., Ltd.), and rosuvastatin calcium (5 mg/kg; AstraZeneca, Wuxi, China). In the ACT group, the mice were intraperitoneally injected with toyocamycin (MedChemExpress, Shanghai, China), 1 mg/kg for a dose, once a week for 8 weeks. The mice were weighed once a week, and FBG levels were measured every 2 weeks.

Oil red O staining

Oil red O staining was performed to quantify lipid accumulation as previously described[21]. For oil red O staining of the aortic root, mouse aorta was collected and fixed with 4% paraformaldehyde. The aorta was dehydrated, trimmed, and embedded with an optimal cutting temperature compound (OCT) embedding matrix; thereafter, the aorta was serially sectioned (10 μm) on a –20°C cryostat and stained. The positive area of staining was determined using ImageJ software (V1.8.0, Bethesda, Maryland, USA).

For gross staining, aortas were fixed with 4% paraformaldehyde, washed with distilled water, and rinsed with 60% isopropyl alcohol. After staining with 60% oil red O, the samples were differentiated using 60% isopropyl alcohol. The residual liquid on the surface was dried and the aorta was fixed with vascular needles to facilitate observation and photograph acquisition.

Hematoxylin and eosin (H&E) and Masson's trichome staining

As previously described[22], morphological analysis of the aortic root lesions was performed using H&E staining, and the extent of collagen fibrosis was determined using Masson's trichome staining. Briefly, the aortic root was fixed with 4% paraformaldehyde, embedded in paraffin wax, routinely deparaffinized and rehydrated, and serially sectioned from the proximal end into 4-μm-thick sections. Subsequently, the sections were deparaffinized and hydrated for Masson's trichrome and H&E staining. The images were captured using an inverted microscope. Thereafter, the sections were visualized using ImageJ software.

Enzyme-linked immunosorbent assay (ELISA)

Interleukin-1 beta (IL-1β; WZ094J4T1875), IL-6 (WZ080HBN0611), and tumor necrosis factor-alpha (TNF-α; WZ054R2V8075) ELISA Kits (Elabscience, Wuhan, China) were used to determine the serum levels of IL-6, IL-1β, and TNF-α in mice. The instruction manual of the manufacturer for the respective kits contains detailed procedures.

Serum biochemical analysis

The blood glucose levels of mice injected with STZ were measured regularly using an electronic blood glucose meter (Accu-Chek, Shanghai, China). Serum levels of total cholesterol (TC), low-density lipoprotein cholesterol (LDL-C), high-density lipoprotein cholesterol (HDL-C), and triglycerides (TG) were measured using a fully automated biochemical analyzer (Toshiba, Tokyo, Japan).

Cellular experiments

HUVECs were purchased from Wuhan Pricell Biomedical Technology Co. (Wuhan, China). As previously described[23], static culture of HUVECs was performed using Dulbecco's modified eagle medium (DMEM; containing 10% fetal bovine serum, 100 U/mL penicillin, and 100 μg/mL streptomycin) in a warm incubator at 5% CO_2 and 37°C. HGHF medium, containing 40 mmol/L glucose and 100 μmol/L sodium palmitate, was used to mimic the HGHF environment *in vitro*, and IR was induced *via* insulin intervention. Well-grown cells in the logarithmic growth phase were inoculated in culture plates for 24 h, and the adhesion of HUVECs was observed. The well-grown cells were divided into the following seven groups: blank control group (Con), normoxic control group (IN), intermittent hypoxia model group (IH), high-dose TMP group (TMPH), low-dose TMP group (TMPL), IRE1α-XBP1 pathway inhibitor-4μ8C group (ACT group), and TMP combined inhibitor group (TMPC). It is noteworthy that, due to the identical intervention drugs used, some group names coincide with those in the mice groupings. However, the intervention methods differ between cells and mice. Please pay attention to this distinction. Except for the Con group, which was replaced with conventional DMEM complete medium, all other wells were replaced with HGHF medium and placed in a cell incubator at 5% CO_2 and 37°C for static culture. After the cells were induced with HGHF medium for 24 h, insulin was added to all groups, except the Con group, for 30 min. Thereafter, 2 mM of TMP, 0.5 mM of TMP, 100 μM of 4μ8C (MedChemExpress), and 100 μM of 4μ8C + 1 mM of TMP were added to the TMPH, TMPL, ACT, and TMPC groups, respectively. The cells were cultured in an incubator for 24 h. Cells from all groups, except the Con and IN groups, were placed in a hypoxia device (MIC-101, Billups-RothenbergSan Diego, California, USA) for 8 h of IH intervention. After

the intervention, the cell culture plates were placed into the incubator for continued culturing for 6 h.

Transmission electron microscopy (TEM) observation of autophagy

A transmission electron microscope (HITACHI, Tokyo, Japan) was used to observe autophagosomes and autolysosomes in each group of cells[24]. HUVECs were fixed with glutaraldehyde and stored in the refrigerator at 4°C overnight. Thereafter, the cells were removed, rinsed, and fixed with osmic acid. The samples were dehydrated and embedded at different temperatures using different concentrations of acetone. Samples were sectioned using an ultrathin microtome and sequentially stained with uranyl acetate and lead citrate. After staining, sections were washed with distilled water, dried, placed on copper grids in a specimen box, and stored at room temperature. Afterward, the sections were photographed using TEM for image collection.

Cell scratch assay

HUVECs were seeded in six-well plates (1×10^6/well). After 24 h of plate culture, DMEM complete medium was added to the Con group and HGHF medium was added to all other wells for 24 h of culture, followed by 30 min of insulin intervention. Two scratches were made perpendicular on the plate, and a marking line was made using a sterile pipette tip (200 μL). The medium in the wells was aspirated and discarded, and detached cells were washed with phosphate-buffered saline (PBS). The medium in the Con group was replaced with a serum-free medium, and HGHF medium and insulin were added to the remaining groups. After 30 min of induction, the corresponding drugs were added to the TMPH, TMPL, ACT, and TMPC groups and photographs were taken to serve as control at 0 h. The plates were then placed into an incubator or hypoxic chamber to culture the cells for 48 h. Thereafter, the cells were observed and photographed under the same microscope at the same position to calculate the migration distance of the cells. The intergroup differences were also calculated. Three parallel wells were used for each group.

CCK-8 assay to determine the inhibition rate of cell proliferation

HUVECs were seeded in 96-well plates (5×10^3 cells/well). After cell adherence was complete, the corresponding medium and different drugs were added to the experimental groups. A blank group containing only the regular culture medium was used, and three replicate wells were used for each group. The plates were placed in an incubator or hypoxic chamber for 24 h. The supernatant was aspirated and discarded and the cells were washed with PBS. Next, 100 μL of the previously prepared CCK-8 solution (protected from light, DMEM serum-free medium: CCK-8 solution = 9:1) was added to each well, and the plates were placed in the corresponding cell culture incubator or hypoxic chamber for real-time observation of the color of the cell culture plate. The cell culture plate with the best color was selected and analyzed using a full-spectrum microplate spectrophotometer (wavelength, 450 nm) to measure the absorbance value (OD value) of each well for cell activity assessment.

Glucose oxidase-peroxidase (GOD-POD) assay

After pharmacological and intermittent hypoxic interventions, the supernatant of cells from each well was collected for centrifugation (1,000 rpm, 5 min), and the glucose concentration in the supernatant of each group of cells was measured using a glucose assay kit (Solarbio, Beijing, China) to assess the glucose use in each group of cells.

The operation steps were as follows:

[1] A working solution was prepared by homogeneously mixing reagents R1 and R2 (R1:R2 = 4:1).
[2] The standard, sample to be tested, and working solution were added sequentially.
[3] Incubate all tubes at 37°C for 20 min. Use the double-distilled water (ddH_2O) blank tube to zero the spectrophotometer. Preheat the spectrophotometer and adjust the wavelength to 505 nm, and the OD value of each tube was determined at 505 nm.
[4] A standard curve was plotted according to the obtained data, and the glucose concentration in the medium was calculated.

$$\text{Glucose concentration (mmol/L)} = \text{standard concentration} \times (OD_{\text{sample tube}} - OD_{\text{blank tube}}) / (OD_{\text{standard tube}} - OD_{\text{blank tube}}).$$

Western blotting

Arterial tissues or cells were lysed with RIPA lysis buffer (Beyotime, Shanghai, China) on ice, and the protein concentration of the lysate was determined using a BCA protein quantification kit (NCM Biotechnology Co., Ltd., Suzhou, China). Thereafter, the product was subjected to sodium dodecyl sulfate-polyacrylamide gel electrophoresis and membrane transfer. The membrane was blocked with 5% skim milk for at least 60 min. The blocking buffer was discarded and the membrane was incubated with the primary antibody overnight. The next day, the membrane was incubated with a horseradish peroxidase-labeled secondary antibody for 60 min at room temperature. Protein signals were detected using an enhanced chemiluminescence solution (Perkin Elmer, Commonwealth of Massachusetts, USA), imaged using a Tanon multifunctional imaging system (Shanghai Tanon Science & Technology Co., Ltd., Shanghai, China), and processed and analyzed using ImageJ software. The details of the antibodies used for western blotting are presented in Table 1.

Statistical analysis

All experimental results were collated, and the data were analyzed and plotted using GraphPad Prism (V9.5.0) and ImageJ software. Data were expressed as means ± standard error (mean ± SEM). For normally distributed data, the *t* test or one-way analysis of variance was used for statistical analysis. Meanwhile, for data without a normal distribution, the Mann-Whitney *U* test or Kruskal–Wallis test was used for statistical analysis. Differences were considered statistically significant at $P < 0.05$.

Table 1

Primary antibodies for western blotting

Antibody	Art. no.	Supplier	Dilution
Anti-IRE1α	ab37073	Abcam	1:10,000
Anti-LC3A	ab52628	Abcam	1:10,000
Anti-Beclin1	ab62557	Abcam	1:10,000
Anti-XBP1s	54351-2	SAB	1:10,000
Anti-XBP1u	AF8367	Beyotime	1:10,000
Anti-LC3B	ab192890	Abcam	1:10,000
Anti-ATF6	ab37149	Abcam	1:10,000
Anti-PERK	ab229912	Abcam	1:10,000

Results

TMP attenuates glucose and lipid metabolism disorders and inflammatory responses in mice with DM and CIH

To determine the effects of CIH on glucose and lipid metabolism disorders in DM mice and the interventional effects of TMP, a DM-AS mouse model was first constructed using STZ combined with a high-fat diet, followed by 8-week CIH intervention and TMP treatment, with rosuvastatin as a positive drug control (Figure 1A). The results showed that the FBG levels of DM mice were significantly increased compared to those of CON mice (Figure 1B, C, Additional File 1, https://links.lww.com/AHM/A171, $P < 0.001$), and the FBG levels further increased after the combined CIH intervention (Figure 1C, $P < 0.001$), accompanied by an increase in the HOMA-IR level (Figure 1D, $P < 0.05$). Oral administration of TMP, toyocamycin, and rosuvastatin calcium had no significant effect on blood glucose metabolism in the mice (Figure 1B–D, Additional File 1, https://links.lww.com/AHM/A171, $P > 0.05$). In addition, compared with the mice in the CON group, DM mice not only had significant increases in serum TC, TG, and LDL-C levels (Figure 1E–G, $P < 0.001$) and aggravated HDL-C metabolism disorders (Figure 1H, $P < 0.001$) but showed significant elevations in the levels of the inflammatory factors IL-1β, IL-6, and IL-10 (Figure 1I–K, $P < 0.001$). Compared to the DM group, CIH further increased the LDL-C levels in mice (Figure 1G, $P < 0.001$) and aggravated inflammatory response level (Figure 1I–K, $P < 0.001$). TMP and toyocamycin (XBP1 inhibitor) interventions reduced TC, TG, and LDL-C levels (Figure 1E–G, $P < 0.001$). Consistently, the serum levels of inflammatory factors IL-1β, IL-6, and IL-10 were reduced (Figure 1I–K, $P < 0.001$). High-dose TMP demonstrated a significant dose advantage in reducing inflammation (Figure 1I–K, $P < 0.001$). These findings suggest that CIH exacerbated lipid metabolism disorders (with a particularly significant effect on LDL-C) and inflammatory responses in DM-AS mice, and this trend was reversed by treatment with TMP and toyocamycin.

TMP ameliorated CIH-induced AS exacerbation in DM mice

We examined the effects of TMP on AS in DM mice with CIH. As shown in Figure 2 A-E, compared with the CON group, significant stenosis, lipid deposition, and increased collagen fibers were observed in the aortic lumen of DM mice, especially in the aortic root ($P < 0.001$). CIH intervention further aggravated AS lesions in DM mice ($P < 0.001$). After oral administration of TMP, rosuvastatin, and toyocamycin, significant improvement in luminal stenosis and significant decreases in plaque area and deposition of lipid and collagen fibers were observed, with the optimal effect observed for low-dose TMP ($P < 0.001$). These findings suggest that TMP significantly improved CIH-induced exacerbation of AS in DM mice and had the same effect as toyocamycin and rosuvastatin.

TMP attenuates enhanced aortic ERS and excessive autophagy in DM mice with CIH by inhibiting XBP1 splicing

The aforementioned results suggest that TMP improved the exacerbation of AS in DM mice with CIH, similar to the effect of toyocamycin, an inhibitor of the classical ERS pathway, the IRE1α-XBP1 pathway. Previous studies have reported ERS overactivation and autophagy inhibition during DM-AS onset. ERS is an important factor in vascular endothelial damage, inducing endothelial dysfunction and accelerating the onset and development of DM-AS through various pathways[25–26]. Moreover, ERS can directly or indirectly regulate autophagy, and the relationship between them is one of the most important targets for the prevention and treatment of AS in recent years[27]. We speculated that the vasoprotective effect of TMP is related to the relationship between ERS and autophagy. Therefore, the expression levels of ERS-related proteins IRE1α, XBP1s, and XBP1u, as well as autophagy-related proteins LC3A, LC3B, and Beclin1 in the aortic tissues of mice, were examined. The results showed that CIH intervention significantly upregulated the expression levels of ERS-related proteins IRE1α and XBP1s (Figure 3A–C, $P < 0.05$ or $P < 0.01$) and autophagy-related proteins LC3A and Beclin1 (Figure 3A, E, and G, $P < 0.01$) but had no significant effect on LC3B expression (Figure 3F). After treatment with different doses of TMP, toyocamycin, and rosuvastatin calcium, the expression levels of XBP1s, LC3A, and Beclin1 were significantly inhibited in mice (Figure 3A, C, E, G; $P < 0.05$, or $P < 0.01$); besides, the expression level of LC3B was significantly reduced by toyocamycin and rosuvastatin. These findings suggest that CIH may activate the IRE1α-XBP1 signaling pathway and promote XBP1 splicing to induce ERS, thereby further triggering excessive autophagy. TMP alleviates the enhanced ERS induced by combined CIH and DM and reduces excessive autophagy by inhibiting XBP1 splicing, eliciting an effect similar to that of the XBP1 inhibitor toyocamycin.

TMP ameliorates exacerbated cell damage in HUVECs induced by IH and HGHF

AS is characterized by endothelial lipid deposition in the arteries, atheromatous plaque formation, and endothelial fibrosis, leading to arterial wall thickening, stiffening, and lumen narrowing, ultimately resulting in ischemic lesions in the heart and brain. HGHF-induced endothelial cell dysfunction is the starting point of DM-AS[28]. For a more precise assessment of the role of TMP, an

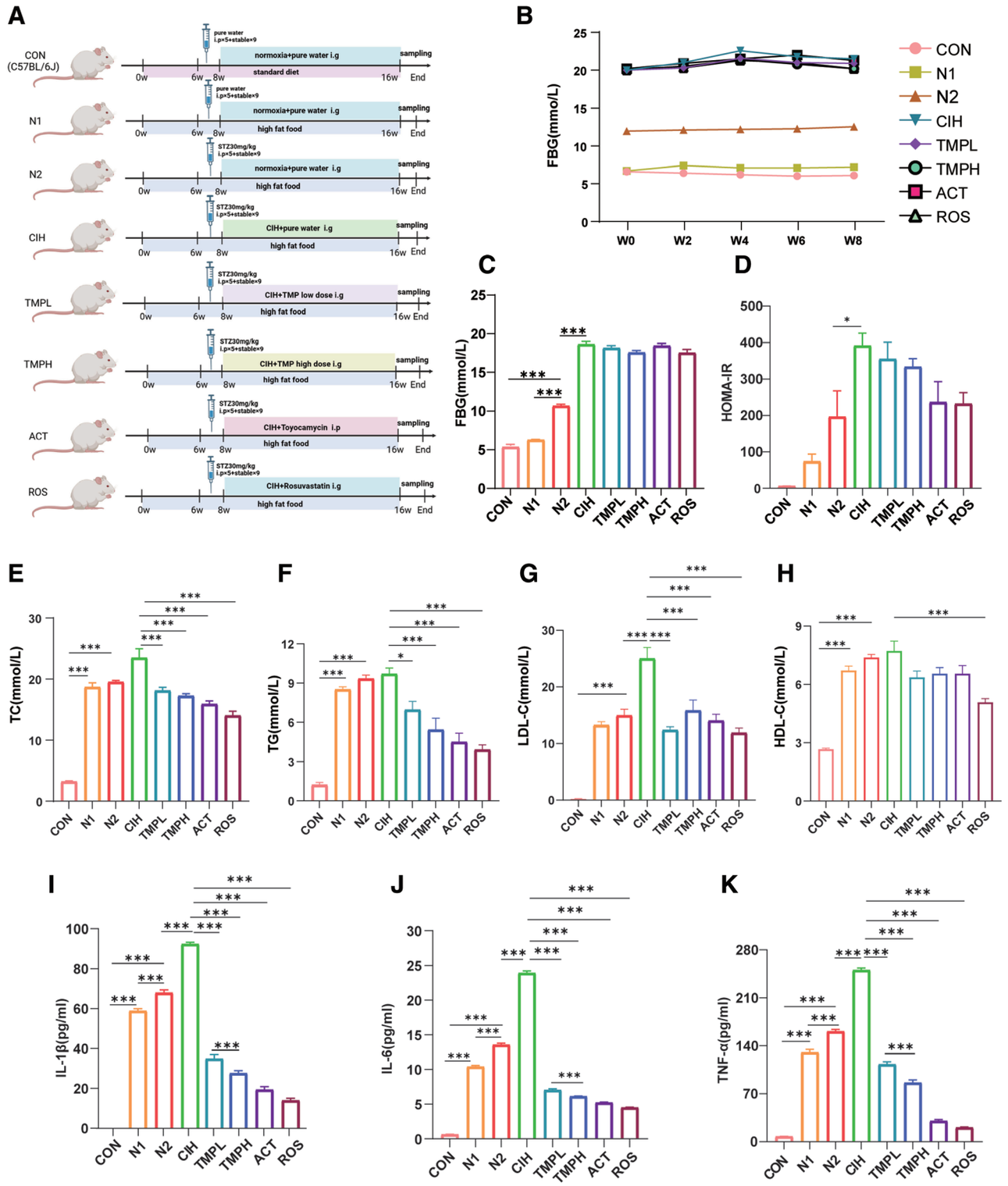


Figure 1. TMP attenuated glucose and lipid metabolism disorders and inflammation in mice with CIH. (A) Flowchart of animal experiments; (B) Line chart of FBG changes in mice at different time periods (n = 8–12); (C) Bar chart of the final blood glucose level in each mice group (n = 8–12); (D) Bar chart of HOMA-IR in each mice group (n = 4); (E) Bar chart of TC levels in each mice group (n = 5); (F) Bar chart of TG levels in each mice group (n = 5); (G) Bar chart of LDL-C levels in each group of mice (n = 5); (H) Bar chart of HDL-C levels in each mice group (n = 5); (I) Bar chart of IL-1β levels in each group of mice (n = 7); (J) Bar chart of IL-6 levels in each group of mice (n = 5); (K) Bar chart of TNF-α levels in each mice group (n = 5). Recorded from the first day after successful DM modeling as W0. *P < 0.05, ***P < 0.001. ACT: Toyocamycin group; CIH: CIH model group; CON: Blank control group; DM: Diabetes mellitus; FBG: Fasting blood glucose; HDL-C: High-density lipoprotein cholesterol; HOMA-IR: Homeostasis Model Assessment of Insulin Resistance; IL-1β: Interleukin-1 beta; LDL-C: Low-density lipoprotein cholesterol; N1: Normoxic control group 1; N2: Normoxic control group 2; ROS: Rosuvastatin group; TG: Triglycerides; TMPH: High-dose TMP group; TMPL: Low-dose TMP group; TNF-α: Tumor necrosis factor-alpha.

HGHF-IR endothelial cell injury model induced by 48 h of HGHF medium combined with insulin treatment was established; this allowed the observation of the effects of IH treatment and intervention with different TMP doses on endothelial cell injury (Figure 4A). The results showed that the cells in the Con group had a

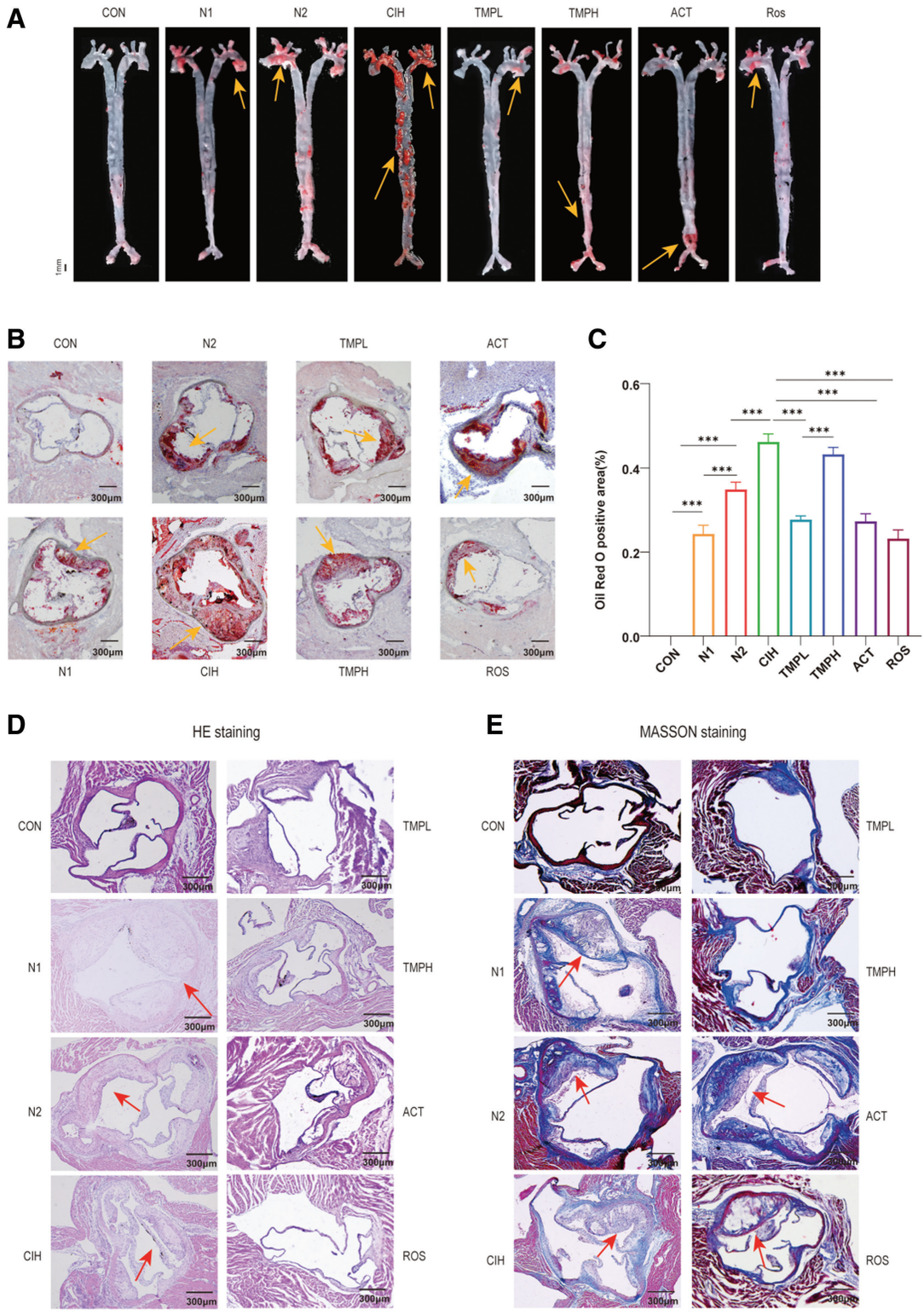


Figure 2. Effect of TMP on CIH-induced AS in DM mice. (A) Oil red O staining of mouse aortic sinus in each group (40×); (B) aortic gross oil red O staining of mice in each group; (C) Bar chart of the positive area of oil red O staining of aortic sinus of mice in each group ($n = 3$); (D) H&E staining of mouse aorta in each group (40×) (red arrows refer to plaque deposition in the mouse aortic lining); (E) Masson's trichome staining of mouse aorta in each group (40×) (red arrows refer to the proliferation and distribution of fibrous connective tissue in the aorta). ***$P < 0.001$. ACT: Toyocamycin group; AS: Atherosclerosis; CIH: CIH model group; CON: Blank control group; DM: Diabetes mellitus; H&E: Hematoxylin and eosin; ROS: Rosuvastatin group; TMP: Tetramethylpyrazine; TMPH: High-dose TMP group; TMPL: Low-dose TMP group.

normal morphology, were mostly cobblestone-shaped, and were arranged in a tight and orderly manner. After the administration of the combined HGHF and insulin treatment, the cell count was reduced and the cells were loosely arranged. The combined IH intervention led to the aggravation of crenation and disorganization, with obvious morphological damages. Moreover, the number of floating cells increased (Figure 4B). TMP intervention significantly improved the cell morphology and restored the cells to a long spindle shape. Furthermore, CCK-8 results demonstrated that (Figure 4C) the inhibition rate of cell proliferation in the IN group increased

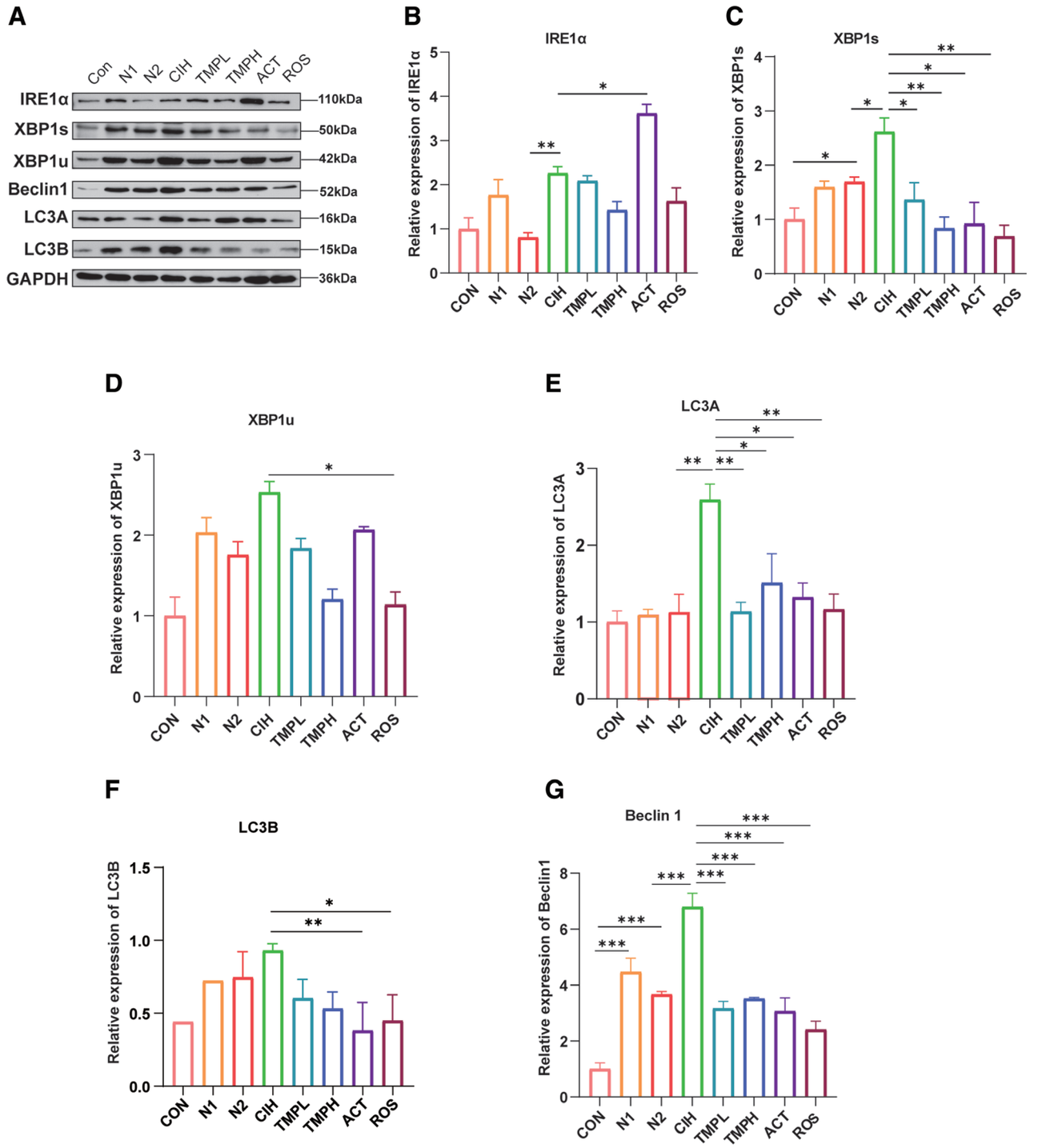


Figure 3. TMP attenuated enhanced aortic ER stress and excessive autophagy in mice with DM and CIH. (A) Representative protein blotting images of aortic IRE1α, XBP1s, XBP1u, LC3A, LC3B, and Beclin1 expression levels in each mice group; (B) quantitative analysis of IRE1α expression in (A); (C) Quantitative analysis of XBP1s expression in (A); (D) Quantitative analysis of XBP1u expression in (A); (E) Quantitative analysis of LC3A expression in (A); (F) Quantitative analysis of LC3B expression in (A); (G) Quantitative analysis of Beclin1 expression in (A). *P < 0.05, **P < 0.01, ***P < 0.001. ACT: Toyocamycin group; CIH: CIH model group; CON: Blank control group; DM: Diabetes mellitus; ER: Endoplasmic reticulum; ROS: Rosuvastatin group; TMP: Tetramethylpyrazine; TMPH: High-dose TMP group; TMPL: Low-dose TMP group.

significantly (P < 0.001) and IH intervention further inhibited proliferative activity (P < 0.001). Moreover, different concentrations of TMP and TMP combined with the inhibitor significantly reduced the proliferation inhibition rate and restored the proliferative activity of the cells (P < 0.001).

In addition, scratch and cell supernatant glucose content assays were performed to observe the effects of TMP on endothelial cell function. Compared with the Con group, the migration distance of the cells in the IN group was significantly shortened (Figure 4D, E, P < 0.05); furthermore, the residual glucose content of the cell supernatant was significantly increased (Figure 4F, P < 0.001). Compared with IN group, IH intervention further shortened the migration distance (Figure 4D, E, P < 0.05), while increasing the residual glucose in the

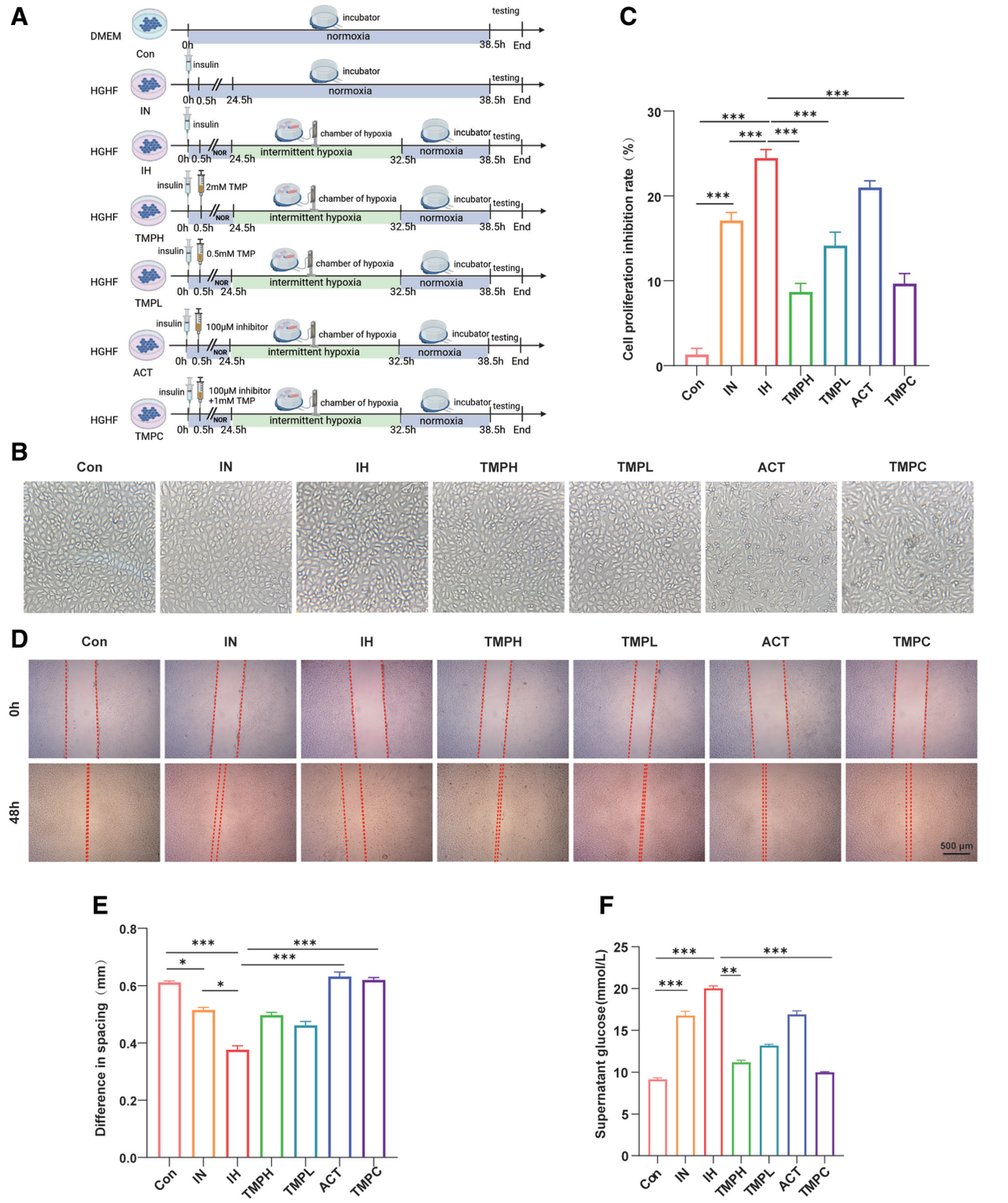


Figure 4. TMP ameliorated exacerbated cell damage in HUVECS induced by IH in combination with HGHF. (A) Flowchart of cell experiments; (B) microscopic photographs (10×) of each group of cells after treatment and 48 h of drug administration; (C) CCK-8 assay for cell proliferation inhibition of each group of cells; (D) microscopic photographs (4×) of each group of cells at the starting (0 h) and end points (48 h) of the scratch assay; (E) absolute values of the scratching distances of each group of cells at 0 and 48 h ($n = 3$) ($n = 5$); (F) GOD-POD method to determine the residual glucose content of cell supernatant ($n = 8$).*$P < 0.05$, **$P < 0.01$, ***$P < 0.001$. ACT: 4μ8C group; Con: Blank control group; GOD-POD: Glucose oxidase-peroxidase; HGHF: High glucose and high fat; HUVECs: Human umbilical vein endothelial cells; IH: Intermittent hypoxia model group; IN: Normoxic control group; TMP: Tetramethylpyrazine; TMPH: High-dose TMP group; TMPC: TMP combined inhibitor group; TMPL: Low-dose TMP group.

supernatant to a certain extent; however, there was no statistical significance (Figure 4F, $P > 0.05$). After TMP treatment, the inhibition of cell proliferation was significantly reduced (Figure 4C, $P < 0.001$), cell morphology and migration distance were restored to different degrees (Figure 4B–E), and the residual glucose content in the supernatant was significantly reduced (Figure 4F, $P < 0.01$). The above findings indicate that IH exacerbated

the damage caused by HGHF on cell morphology, migration capacity, proliferation, and glucose consumption, whereas TMP improved these damage.

TMP inhibition of XBP1 splicing ameliorates ERS and excessive autophagy in HUVECs induced by the combination of IH and HGHF

In vivo experiments showed that TMP alleviated the increased ERS and excessive autophagy induced by combined CIH and DM and improved AS in mice by inhibiting XBP1 splicing. To further verify the effects of IH on ERS and autophagy in endothelial cells and determine the intervention targets of TMP, in addition to IRE1α, we examined the expression levels of two other classical ERS pathway proteins, namely PERK and ATF6. The results showed that compared with the IN group, combined IH and HGHF significantly enhanced the expression levels of IRE1α and XBP1s (Figure 5A–C, $P < 0.01$) but had no significant effect on ATF6, PERK and XBP1u (Figure 5D, E, F, $P > 0.05$), indicating that IH induced ERS in endothelial cells mainly through the IRE1α-XBP1s pathway. Meanwhile, compared with the IN group, the expression level of the autophagy-related protein LC3A in IH group was significantly elevated (Figure 5H, $P < 0.05$) but no significant change was observed in Beclin1 expression (Figure 5G, $P > 0.05$). In addition, TEM results showed that IH intervention significantly increased the number of autophagosomes/autolysosomes (Figure 5I). The expression levels of the ERS-related protein XBP1s and autophagy-related proteins Beclin1 and LC3A were significantly downregulated after treatment with different doses of TMP, inhibitors, and their combination (Figure 5C, G, H; $P < 0.05$ or $P < 0.01$), and the number of autophagosomes/autolysosomes was significantly reduced, as seen in microscopic observations (Figure 5I).

Together, these findings indicate that combined IH and HGHF induced severe ERS by activating the IRE1α-XBP1 pathway and enhancing XBP1 splicing. ERS activation further triggered excessive autophagy, which impaired the morphology, migration, and glucose consumption of HUVECs. TMP and IRE1α-XBP1 pathway inhibitor, 4μ8C, inhibited ERS and alleviated the excessive autophagy of cells by suppressing the splicing of XBP1 downstream of IRE1α, thus mitigating the cellular damage caused by IH and HGHF-induced IR.

Discussion

There is a strong association between OSA and DM, which are two important risk factors for AS. A 12.8-year follow-up of a subpopulation participating in the Sleep Heart Health Study and the Atherosclerosis Risk in Communities study revealed that the prevalence of Type 2 Diabetes Mellitus (T2DM) increased with increasing OSA severity[29] Cellular studies have shown that IH induces abnormal islet cell function and triggers DM by downregulating the CD38-cADPR signaling system and upregulating the Reg gene family[30]. Consequently, OSA and DM may independently induce AS, and their intricate interplay can accelerate AS development. However, owing to limited resources in the medical field and the underdevelopment of sleep medicine, the global awareness and diagnosis of OSA remain low. Correspondingly, existing medical research provides limited understanding of the mechanism underlying OSA- and DM-mediated AS development. Furthermore, OSA treatment primarily relies on non-pharmacological therapies, leading to poor patient adherence. Hence, the identification of suitable therapeutic drugs is a pressing concern in the treatment of OSA and its complications.

L. sinense cv. "Chuanxiong" is a notable Chinese herbal medicine known to promote blood circulation, eliminate blood stasis, and regulate *qi*. Its active ingredients confer the various cardiovascular protective pharmacological effects, such as anticoagulation and vasodilatation, associated with Chuanxiong[14]. TMP is the primary active component of Chuanxiong and is used to treat cardiovascular and cerebrovascular diseases. Furthermore, TMP has shown efficacy in preventing the onset and progression of AS through anti-inflammatory and antioxidant pathways and *via* lipid metabolism enhancement[15]. Numerous studies have highlighted the role of TMP in counteracting IH-induced pathological changes. In mice models, TMP has been demonstrated to mitigate pathological alterations, including the impairment of pulmonary artery endothelial morphology and function induced by CIH, as well as the heightened sensitivity to endothelin-1[31]. Another study demonstrated that TMP ameliorated platelet aggregation and activation, while suppressing the upregulation of the SREBP-1c/FAS pathway in a 3T3-L1 cell model of IH-induced IR. This was achieved by diminishing platelet calcium ion influx and inhibiting the activation of PI3KA/Akt-PI3Kβ. Besides, another study reported that TMP enhances IR and reduces oxidative stress[17].

In the present study, CIH significantly increased the number of AS lesions in DM mice. This led to the exacerbation of glucose and lipid metabolism disorders and an increase in serum levels of inflammatory factors such as IL-1β, IL-6, and TNF-α. In *in vitro* studies, exposure of HUVECs to IH and an HGHF environment resulted in notable changes in cell morphology, decreased proliferation activity, impaired cell migration, and reduced glucose consumption. Treatment with TMP reversed these effects and halted the progression of AS lesions.

As the largest organelle in eukaryotic cells, the endoplasmic reticulum plays an important role in protein synthesis, translation, secretion, as well as cell apoptosis, autophagy, and the regulation of lipid homeostasis[32–33]. Exposure of the endoplasmic reticulum to various internal and external stimuli leads to the disruption homeostasis, and the UPR is activated to alleviate ERS through the transcription and expression of recoded genes. The IRE1α-XBP1 pathway is the most conserved among the three major branches of UPR, playing a crucial role in maintaining endoplasmic reticulum homeostasis and being closely related to glucose and lipid metabolism disorders, obesity, and AS development[34–35].

IRE1α is associated with obesity; diet-induced obesity was alleviated during IRE1α deficiency in the adipose tissues of mice, and the anti-obesity effect of β3 adrenergic receptor agonists was further enhanced[36]. A large amount of XBP1s were found in the AS region of ApoE$^{-/-}$ mice, and the sustained activation of XBP1s promoted the onset and development of AS[37]. In recent

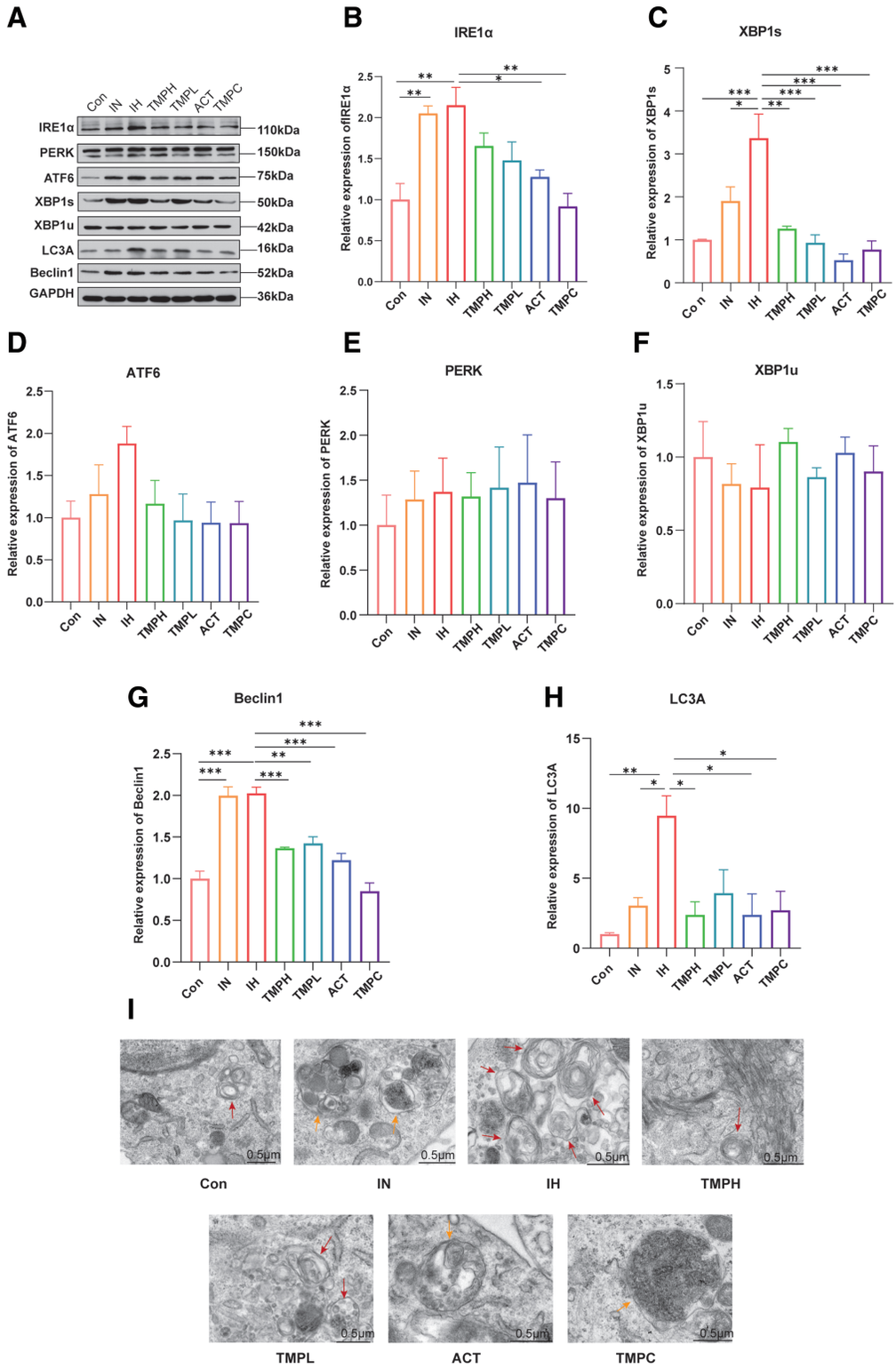


Figure 5. TMP inhibition of XBP1 splicing ameliorated ERS and excessive autophagy in IH- and HGHF-induced HUVECs. (A) Representative protein blotting images of IRE1α, PERK, ATF6, XBP1s, XBP1u, LC3A, and Beclin1 expression levels in each group of cells; (B) Quantitative analysis of IRE1α expression in (A); (C) Quantitative analysis of XBP1s expression in (A); (D) Quantitative analysis of ATF6 expression in (A); (E) Quantitative analysis of PERK expression in (A); (F) Quantitative analysis of XBP1u expression in (A); (G) Quantitative analysis of Beclin1 expression in (A); (H) Quantitative analysis of LC3A expression in (A); (I) TEM to observe the changes of autophagosomes and autolysosomes in cells of each group (×20k). *P < 0.05, **P < 0.01, ***P < 0.001. ERS: Endoplasmic reticulum stress; HGHF: High glucose and high fat; HUVECs: Human umbilical vein endothelial cells; IH: Intermittent hypoxia model group; PERK: Protein kinase R-like endoplasmic reticulum kinase; TEM: Transmission electron microscopy; TMP: Tetramethylpyrazine.

years, the complex interactions between autophagy and ERS have become a research hotspot, offering a new direction for studying the underlying mechanisms and treatments of AS[38].

In endothelial cells, sustained activation of XBP1 mRNA splicing induced the formation of autophagosomes, possibly due to XBP1s directly binding to a part of the promoter of the autophagy gene Beclin1.

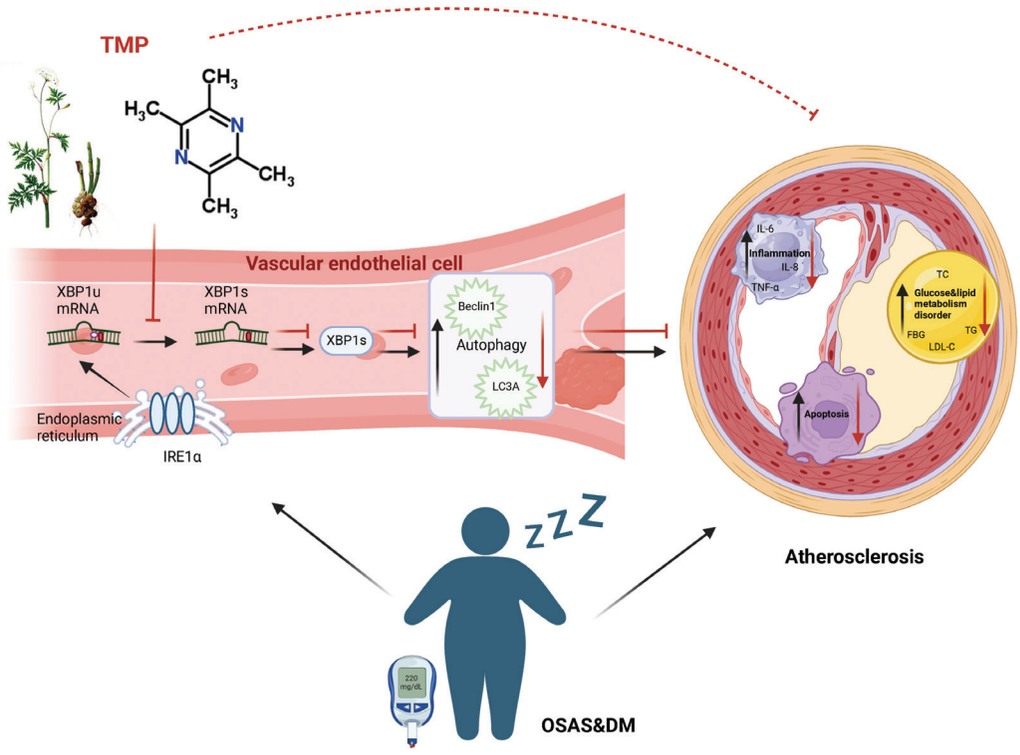


Figure 6. Mechanisms by which TMP attenuates IH-induced endothelial damage and atherosclerosis in DM vessels. In patients with both OSA and DM, IRE1α, a transmembrane protein present in the endoplasmic reticulum, is significantly activated. When it is phosphorylated, it catalyzes the shearing of XBP1 mRNA, transforming it from XBP1u to functionally active XBP1s, which can further contribute to the development of AS by promoting cellular autophagy, and further promoting pathological responses such as inflammation, apoptosis, and glycolipid metabolism disorders. The active molecule TMP of Chuanxiong, a traditional Chinese medicine efficacious in activating blood circulation and removing blood stasis, can inhibit the shearing of XBP1, that is, the transformation of XBP1u into XBP1s, thus inhibiting the enhancement of cellular autophagy and the related pro-AS pathological reactions and achieving the therapeutic effect of anti-AS. AS: Atherosclerosis; DM: Diabetes mellitus; IH: Intermittent hypoxia model group; OSA: Obstructive sleep apnea; TMP: Tetramethylpyrazine.

This action activated transcription and further triggered autophagy in endothelial cells. XBP1 overexpression led to increased expression of Beclin1, whereas XBP1-induced autophagy disappeared upon Beclin1 knockout[11].

In the present study, after CIH treatment, the expression levels of the ERS-related protein XBP1s and autophagy-related proteins Beclin1 and LC3A were upregulated in the endothelial cells of mice with diabetes, resulting in significant aggravation of aortic AS lesions and cellular damage. This suggests that CIH exacerbates endothelial cell damage and AS by promoting ERS and excessive autophagy. Following TMP treatment, the expression levels of mouse aortic XBP1s and two autophagy-related proteins, namely Beclin1 and LC3A, were significantly inhibited. In addition, *in vitro* experiments revealed that TMP inhibited the enhanced expression of XBP1s, LC3A, and Beclin1 induced by IH in endothelial cells, achieving similar effects as that of the pathway inhibitor 4μ8C. However, the results for the ATF6 and PERK pathways were negative. These findings demonstrated that the amelioration of vascular endothelial injury and diabetes-associated AS by TMP was mainly achieved through the regulation of the interaction between the IRE1α-XBP1 pathway and autophagy.

Furthermore, in this study, *in vivo* and *in vitro* experiments demonstrated that TMP attenuated glucose and lipid metabolism disorders as well as inflammatory responses in mice induced by combined CIH and DM. This was achieved by regulating the interaction between the IRE1α-XBP1 signaling pathway and autophagy, consequently ameliorating endothelial cell injury and DM-AS progression (Figure 6). Notably, in the present study, the knocking down of signaling molecules such as IRE1α, XBP1, and Beclin1 was not conducted to further validate the role of these pathways in CIH-induced DM-AS. Further investigation is, therefore, necessary in the future.

Conclusion

This study revealed that TMP ameliorated CIH-mediated DM-AS by modulating the interaction between ERS and autophagy through the regulation of the IRE1α-XBP1 signaling pathway. Therefore, in future studies, the use of TMP for the prevention and treatment of OSAS-associated AS should be considered. In addition, new ideas for the management of patients with OSAS combined with DM can be provided.

Conflict of interest statement

The authors declare no conflict of interest.

Funding

The research fund of this project comes from the National Natural Science Foundation of China (82074264).

Author contributions

Yue Liu designed the manuscript. Binyu Luo and Wenting Wang did the literature search, wrote the manuscript, and drafted figures. Yanfei Liu, Yiwen Li, Binyu Luo, and Wenting Wang revised the manuscript. All authors listed have made a substantial contribution to the work. All authors have read and approved the article.

Ethical approval of studies and informed consent

This animal study was approved by the Animal Ethics Committee of Xiyuan Hospital, China Academy of Chinese Medical Sciences (2021XLC046-1).

Acknowledgments

None.

Data availability

The datasets used and/or analyzed during the current study are available from the corresponding author on reasonable request.

References

[1] Marin JM, Carrizo SJ, Vicente E, et al. Long-term cardiovascular outcomes in men with obstructive sleep apnoea-hypopnoea with or without treatment with continuous positive airway pressure: an observational study. *Lancet (London)* 2005;365(9464):1046–1053.
[2] Yaggi HK, Concato J, Kernan WN, et al. Obstructive sleep apnea as a risk factor for stroke and death. *N Engl J Med* 2005;353(19):2034–2041.
[3] De Vega Sánchez B, Juarros Martínez SA, Del Olmo Chiches M, et al. Obstructive sleep apnoea, type 2 diabetes and cardiovascular risk factors. *Eur J Intern Med* 2017;39:e16–e17.
[4] Huang T, Lin BM, Stampfer MJ, et al. A population-based study of the bidirectional association between obstructive sleep apnea and type 2 diabetes in three prospective U.S. cohorts. *Diabetes Care* 2018;41(10):2111–2119.
[5] Muraki I, Wada H, Tanigawa T. Sleep apnea and type 2 diabetes. *J Diabetes Investig* 2018;9(5):991–997.
[6] Trzepizur W, Le Vaillant M, Meslier N, et al. Independent association between nocturnal intermittent hypoxemia and metabolic dyslipidemia. *Chest* 2013;143(6):1584–1589.
[7] Ma L, Zhang J, Qiao Y, et al. Intermittent hypoxia composite abnormal glucose metabolism-mediated atherosclerosis in vitro and in vivo: the role of SREBP-1. *Oxid Med Cell Longev* 2019;2019:4862760.
[8] Tian J, Yue L, Lizhi L, et al. Endoplasmic reticulum stress and autophagy: a potential therapeutic target for atherosclerosis. *Life Sci* 2017;29(4):356–363.
[9] Tufanli O, Telkoparan Akillilar P, Acosta-Alvear D, et al. Targeting IRE1 with small molecules counteracts progression of atherosclerosis. *Proc Natl Acad Sci USA* 2017;114(8):E1395–E1404.
[10] Huang S, Xing Y, Liu Y. Emerging roles for the ERS sensor IRE1α in metabolic regulation and disease. *J Biol Chem* 2019;294(49):18726–18741.
[11] Margariti A, Li H, Chen T, et al. XBP1 mRNA splicing triggers an autophagic response in endothelial cells through BECLIN-1 transcriptional activation. *J Biol Chem* 2013;288(2):859–872.
[12] Tian PG, Jiang ZX, Li JH, et al. Spliced XBP1 promotes macrophage survival and autophagy by interacting with Beclin-1. *Biochem Biophys Res Commun* 2015;463(4):518–523.
[13] Chen HR. *Cluster Analysis of Traditional Chinese Medicine Syndrome of Obstructive Sleep Apnea Hypopnea Syndrome Combined with Type 2 Diabetes Mellitus and its Correlation with Insulin Resistance*. Fujian University of Chinese Medicine,2019.
[14] Xudong Z, Lu H. Value of thrombologram in type 2 diabetes mellitus patients with obstructive sleep apnea hypopnea syndrome. *J Clin Med Lit Electron* 2018;5(6):6–8.
[15] Guo M, Liu Y, Shi D. Cardiovascular actions and therapeutic potential of tetramethylpyrazine (active component isolated from Rhizoma Chuanxiong): roles and mechanisms. *Biomed Res Int* 2016;2016:2430329.
[16] Zhao Y, Liu Y, Chen K. Mechanisms and clinical application of tetramethylpyrazine (an Interesting Natural Compound Isolated from Ligusticum Wallichii): current status and perspective. *Oxid Med Cell Longevity* 2016;2016:2124638.
[17] Ma L, Zhang J, Liu Y, et al. Intervention effects of qi-benefiting and blood-activating traditional Chinese medicine combinations on Sterol regulatory element-binding protein 1c/Fatty acid synthase (SREBP-1c/FAS) signaling pathway in an intermittent hypoxia-complex insulin resistance cell model. *World Sci Technol Modernization Tradit Chin Med* 2019;21(11):2516–2525.
[18] Sun WT, Wang XC, Novakovic A, et al. Protection of dilator function of coronary arteries from homocysteine by tetramethylpyrazine: role of ERS in modulation of BKCa channels. *Vascul Pharmacol* 2019;113:27–37.
[19] Jiang K, Xu Y, Wang D, et al. Cardioprotective mechanism of SGLT2 inhibitor against myocardial infarction is through reduction of autosis. *Protein Cell* 2022;13(5):336–359.
[20] Asaf R, Blum S, Roguin A, et al. Haptoglobin genotype is a determinant of survival and cardiac remodeling after myocardial infarction in diabetic mice. *Cardiovasc Diabetol* 2009;8:29.
[21] Andrés-Manzano MJ, Andrés V, Dorado B. Oil Red O and hematoxylin and eosin staining for quantification of atherosclerosis burden in mouse aorta and aortic root. *Methods Mol Biol* 2015;1339:85–99.
[22] Zhu J, Liu B, Wang Z, et al. Exosomes from nicotine-stimulated macrophages accelerate atherosclerosis through miR-21-3p/PTEN-mediated VSMC migration and proliferation. *Theranostics* 2019;9(23):6901–6919.
[23] Wang W, Wang S, Li Y, et al. Network pharmacology, molecular docking, and in vitro experimental verification of the mechanism of Guanxining in treating diabetic atherosclerosis. *J Ethnopharmacol* 2024;324:117792.
[24] Zhang Y, Liu D, Hu H, et al. HIF-1α/BNIP3 signaling pathway-induced-autophagy plays protective role during myocardial ischemia-reperfusion injury. *Biomed Pharmacother* 2019;120:109464.
[25] Dong Y, Fernandes C, Liu Y, et al. Role of endoplasmic reticulum stress signalling in diabetic endothelial dysfunction and atherosclerosis. *Diab Vasc Dis Res* 2017;14(1):14–23.
[26] Galán M, Kassan M, Kadowitz PJ, et al. Mechanism of endoplasmic reticulum stress-induced vascular endothelial dysfunction. *Biochim Biophys Acta* 2014;1843(6):1063–1075.
[27] Yao ST, Qin SC. The relationship of autophagy with endoplasmic reticulum stress and its role in pathogenesis, prevention and therapy of atherosclerosis. *Sheng Li Xue Bao* 2017;69(4):515–521.
[28] Poznyak A, Grechko AV, Poggio P, et al. The diabetes mellitus-atherosclerosis connection: the role of lipid and glucose metabolism and chronic inflammation. *Int J Mol Sci* 2020;21(5):1835.
[29] Nagayoshi M, Punjabi NM, Selvin E, et al. Obstructive sleep apnea and incident type 2 diabetes. *Sleep Med* 2016;25:156–161.
[30] Ota H, Fujita Y, Yamauchi M, et al. Relationship between intermittent hypoxia and type 2 diabetes in sleep apnea syndrome. *Int J Mol Sci* 2019;20(19):4756.
[31] Zheng L, Zhuo W, Yanzhen G, et al. Study on the protective effect of ligustrazine on intermittent hypoxia-induced pulmonary artery endothelial injury in rats. *World Clin Med* 2016;10(9):1–2.
[32] Metcalf MG, Higuchi-Sanabria R, Garcia G, et al. Beyond the cell factory: homeostatic regulation of and by the UPR(ER). *Sci Adv* 2020;6(29):eabb9614.
[33] Hetz C, Zhang K, Kaufman RJ. Mechanisms, regulation and functions of the unfolded protein response. *Nat Rev Mol Cell Biol* 2020;21(8):421–438.
[34] Wu R, Zhang QH, Lu YJ, et al. Involvement of the IRE1α-XBP1 pathway and XBP1s-dependent transcriptional reprogramming in metabolic diseases. *DNA Cell Biol* 2015;34(1):6–18.
[35] Sha H, He Y, Yang L, et al. Stressed out about obesity: IRE1α-XBP1 in metabolic disorders. *Trends Endocrinol Metab* 2011;22(9):374–381.
[36] Chen Y, Wu Z, Huang S, et al. Adipocyte IRE1α promotes PGC1α mRNA decay and restrains adaptive thermogenesis. *Nat Metab* 2022;4(9):1166–1184.
[37] Zeng L, Zampetaki A, Margariti A, et al. Sustained activation of XBP1 splicing leads to endothelial apoptosis and atherosclerosis development in response to disturbed flow. *Proc Natl Acad Sci U S A* 2009;106(20):8326–8331.
[38] Jinfan T, Yue L, Zhi L, et al. Endoplasmic reticulum stress, autophagy and their interaction: a potential new target for the treatment of atherosclerosis. *Life sci* 2017;29(4):356–363.